Chinese Journal of Catalysis 36 (2015) 649–656

available at www.sciencedirect.com

ScienceDirect

journal homepage: www.elsevier.com/locate/chnjc

Article

The effect of Fe species distribution and acidity of Fe-ZSM-5 on the hydrothermal stability and SO_2 and hydrocarbons durability in NH_3-SCR reaction

Xiaoyan Shi *, Hong He, Lijuan Xie

State Key Joint Laboratory of Environment Simulation and Pollution Control, Research Center for Eco-Environmental Sciences, Chinese Academy of Sciences, Beijing 100085, China

ARTICLE INFO

Article history:
Received 4 November 2014
Accepted 12 December 2014
Published 20 April 2015

Keywords:
Iron-ZSM-5
Ammonia selective catalytic reduction
Removal of nitrogen oxide
SO_2 durability
Hydrothermal stability

ABSTRACT

Fe-exchanged ZSM-5 catalysts prepared from Na^+ and H^+ forms of ZSM-5 were evaluated for the selective catalytic reduction of NO_x by NH_3 (NH_3-SCR). Fe-H-ZSM-5 showed higher SCR activity than Fe-Na-ZSM-5 both when fresh and after hydrothermal aging at 750 °C in 5% H_2O/air. The Fe species distribution and acidity of Fe-H-ZSM-5 and Fe-Na-ZSM-5 were found to be different. The dealumination of the zeolite framework of Fe-H-ZSM-5 during hydrothermal aging was found to be more severe compared with that of Fe-Na-ZSM-5. The durability of Fe-H-ZSM-5 and Fe-Na-ZSM-5 in NH_3-SCR was compared using SO_2 tolerance and hydrocarbon resistance experiments. The effect of water and SO_2 on the activity of the two catalysts was similar, such that their activity decreased at low temperatures and increased at high temperatures. Fe-Na-ZSM-5 showed better propene resistance than Fe-H-ZSM-5. The SO_2 and propene poisoning of the two Fe-ZSM-5 catalysts were found to be reversible.

1. Introduction

The selective catalytic reduction (SCR) of NO_x by NH_3 is a well-proven process for the removal of NO_x from stationary and mobile sources. A number of metal-exchanged zeolites (MFI, MOR, BEA, and FER), especially Cu- and Fe-based MFI-structured zeolites (ZSM-5), are active SCR catalysts and have been studied extensively [1,2]. Cu-ZSM-5 catalysts show high activity at low temperatures (< 300 °C), but their hydrothermal stability is limited [2,3]. Fe-ZSM-5 is more attractive for its nontoxic metal use, high activity at high temperature (> 300 °C) and better hydrothermal stability [2,4].

The NH_4^+, H^+, and Na^+ forms of ZSM-5 can be used as parent zeolites for Cu- and Fe-ZSM-5 preparation. The H^+ and Na^+ cocations have been found to influence the catalytic behavior of Cu-zeolite catalysts [5–8]. The Cu location and the redox properties of Cu-zeolite catalysts (Cu-MOR and Cu-FAU) can be affected by co-cations. For example, the Cu in the Na^+ form catalyst has been found to be more easily reduced than that in the protonic form [5,6]. Sultana *et al.* [7,8] reported that Cu-ZSM-5 prepared from a Na^+ form precursor showed higher activity for NH_3-SCR than those prepared from a H^+ form precursor, owing to the existence of a larger number of Cu^+ species and easily reducible Cu^{2+} species in the obtained Cu-NaZSM-5.

Controversial results have been reported for the effect of co-cations on the catalytic performance of Fe-ZSM-5 catalysts. Fe-ZSM-5 prepared from a Na-ZSM-5 precursor showed lower NO conversion in the NH_3-SCR reaction compared with those

* Corresponding author. Tel: +86-10-62911040; Fax: +86-10-62849121; E-mail: xyshi@rcees.ac.cn
This work was financially supported by the National High Technology Research and Development Program of China (863 Program, 2013AA065301) and the National Natural Science Foundation of China (51278486, 51221892).
DOI: 10.1016/S1872-2067(14)60268-0 | http://www.sciencedirect.com/science/journal/18722067 | Chin. J. Catal., Vol. 36, No. 4, April 2015

prepared from H^+ or NH_4^+ forms [9,10]. Pieterse *et al*. [11] pointed out that the removal of framework aluminium by steam-dealumination should be slowed in Fe-ZSM-5 owing to the replacement of protons with sodium. Contrarily, Brandenberger *et al*. [10] reported that hydrothermal deactivation at 800 °C in 10% H_2O/air resulted in a greater decrease in the NH_3-SCR activity of Na-ZSM-5 exchanged Fe-ZSM-5 than H-ZSM-5 exchanged samples, but did not give further explanation.

Hydrothermal stability, hydrocarbon (HC) and SO_2 tolerance are the challenges facing the practical application of de-NO_x SCR catalysts in diesel engines. In this paper, Fe-ZSM-5 catalysts with different Fe species distribution and acidity were prepared from Na^+ and H^+ form ZSM-5 by liquid ion exchange, and their catalytic behavior in the NH_3-SCR reaction was investigated. Temperature-programmed reduction with hydrogen (H_2-TPR), UV-vis diffuse reflectance spectrometry (DRS), in situ diffuse reflectance infrared Fourier transform spectroscopy (DRIFTS), nuclear magnetic resonance (NMR), and X-ray diffraction (XRD) were used to characterize the fresh and hydrothermally aged Fe-ZSM-5 catalysts. The hydrothermal stability, SO_2 and HC resistance of Fe-Na-ZSM-5 and Fe-H-ZSM-5 in the NH_3-SCR reaction were compared and discussed.

2. Experimental

2.1. Catalyst preparation

Na-ZSM-5 with SiO_2/Al_2O_3 = 25 was obtained from Nankai University. The Na-ZSM-5 was mixed with 0.5 mol/L NH_4NO_3 aqueous solution and heated in a water bath at 80 °C for 24 h, followed by washing and filtration. The resultant NH_4-ZSM-5 was dried overnight at 110 °C and then calcined at 550 °C for 6 h in air to obtain H-ZSM-5. Fe-ZSM-5 catalysts were prepared by liquid ion exchange. Typically, 10 g ZSM-5 precursor was added to $FeCl_2{\cdot}4H_2O$ solution (17.8 g/L) with constant stirring under a continuous flow of N_2 (200 mL/min) in a water bath at 80 °C. After 24 h, the mixture was filtered and washed with deionized water. The resulting powder was dried overnight at 110 °C and calcined at 600 °C for 6 h in air to obtain Fe-Na-ZSM-5 and Fe-H-ZSM-5, which are hereafter denoted Fe-NaZ and Fe-HZ, respectively. The hydrothermal aging of Fe-NaZ and Fe-HZ was carried out at 750 °C in 10% H_2O/air for 12 h.

2.2. Catalytic characterization

H_2-TPR experiments were performed with a Micromeritics AutoChem 2920 chemisorption analyzer equipped with a thermal conductivity detector (TCD). For the analysis, 100 mg of powdered sample was pre-treated in 20% O_2 at 550 °C for 20 min. After cooling to 30 °C in Ar, the H_2-TPR measurements were recorded in 10% H_2/Ar (50 mL/min), with a heating rate of 20 °C/min and a final temperature of 900 °C.

UV-Vis DRS spectra were recorded with a Hitachi UV3010 (Japan). $BaSO_4$ was used as the reference material. The Fe-ZSM-5 catalysts were diluted with $BaSO_4$ at a ratio of 1:4. The spectra were converted with the Kubelka-Munk (KM) function for comparison.

In situ DRIFTS experiments of NH_3 adsorption over the Fe-ZSM-5 catalysts were performed on a Fourier transform infrared spectrometer (FTIR; Nicolet Nexus 670). Each sample was pretreated at 550 °C in a flow of 20% O_2/N_2 for 20 min, then purged with pure N_2 for 20 min and cooled to 140 °C in N_2. Then, the samples were exposed to a flow of 1% NH_3/N_2 and the spectra were recorded until NH_3 adsorption saturation.

Powder XRD measurements were carried out on a Panalytical X-ray diffractometer (Netherlands, X'Pert PRO MPD) with a Cu K_α radiation source. The 2θ data from 5° to 60° were collected with a step size of 0.02°.

Solid state ^{27}Al MAS NMR spectra were collected on a Brucker AVANCE III 400MHz WB Solid-State NMR spectrometer. All ^{27}Al MAS NMR spectra were externally referenced to an aqueous solution of $Al(NO_3)_3$ at 0 ppm, and were obtained at a sample spinning rate of 10 kHz using 15° pulses and a 0.5 s recycle delay, a total of 12000 pulses being accumulated.

2.3. Activity tests

The SCR reaction conditions were controlled as follows: 500 ppm NO, 500 ppm NH_3, 5% O_2, 5% H_2O (when used), 100 ppm SO_2 (when used), 500 ppm C_3H_6 (when used), N_2 balance; 50 mg catalyst, total flow rate of 500 mL/min and gas hourly space velocity (GHSV) of 320 000 h^{-1}. The effluent gas was analyzed using an FTIR spectrometer (Nicolet Nexus 670). NO_x conversion (X_{NOx}) was calculated as follows:

$$X_{NOx} = (1 - ([NO] + [NO_2])_{out}/([NO] + [NO_2])_{in}) \times 100\%$$

3. Results and discussion

3.1. Catalyst composition

The elemental composition of the samples was analyzed using an inductively coupled plasma optical emission spectrometer (ICP-OES). Although the two catalysts were prepared by exactly the same procedure, the Fe loading of Fe-NaZ (1.62 wt%) was higher than that of Fe-HZ (1.27 wt%). Similar results have been reported and explained to be caused by the fact that the change in solution pH during the ion exchange process might be different for different precursors [9]. The residual Na content in Fe-NaZ was 0.61 wt%.

3.2. H_2-TPR results

The H_2-TPR profiles obtained from fresh and hydrothermally aged Fe-HZ and Fe-NaZ are shown in Fig. 1(a). A mechanical mixture of 5 wt% α-Fe_2O_3 with H-ZSM-5 was prepared and tested for comparison. The H_2-TPR profile of 5 wt% α-Fe_2O_3/H-ZSM-5 showed broad reduction features between 325–650 °C. This suggests that the reduction of iron oxide particles completed below 650 °C, by the reduction of Fe_2O_3 to Fe_3O_4 and then reduction of FeO_x to Fe^0 via FeO [10,12–16]. According to previous work on the H_2-TPR of Fe-ZSM-5 catalysts, the first reduction peak corresponds to the reduction of

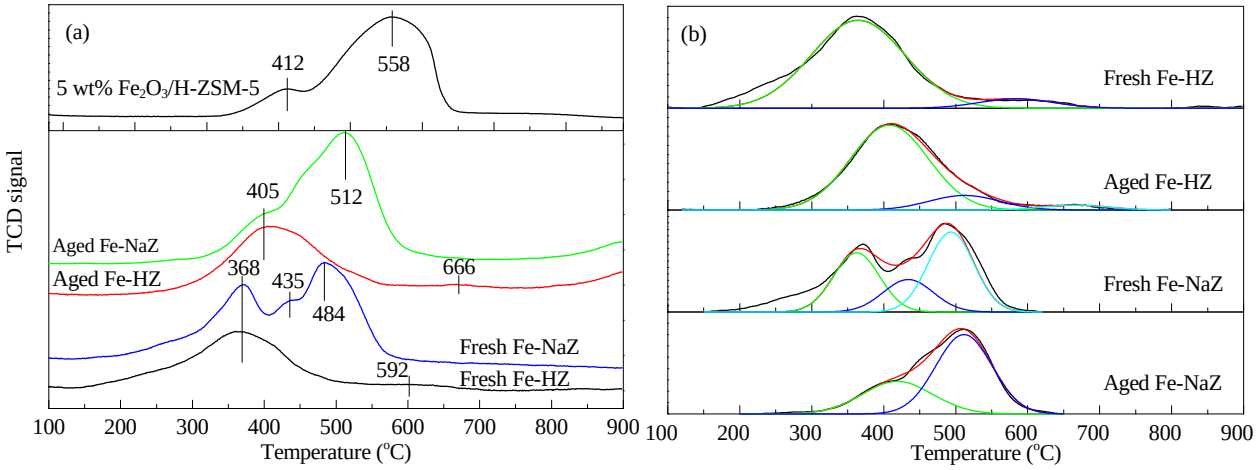

Fig. 1. (a) H_2-TPR profiles of fresh and hydrothermally aged Fe-HZ and Fe-NaZ; (b) Deconvoluted sub-bands of the H_2-TPR profiles.

Fe^{3+} to Fe^{2+} [10,12–16]. When Fe^{3+} is located at ion-exchanged positions, further reduction of Fe^{2+} to Fe^0 occurs at temperatures above 1000 °C owing to the collapse of the zeolite framework [10,12].

As shown in Fig. 1(a), the H_2-TPR profile of fresh Fe-HZ exhibited one main reduction peak at 370 °C, which can be assigned to the reduction of Fe^{3+} to Fe^{2+}. No significant reduction peaks were observed from 550 °C to 900 °C in the profile of Fe-HZ, which indicates that most of the iron in Fe-HZ was located at exchange sites [13,14]. The first peak in the H_2-TPR profile of fresh Fe-NaZ can be also attributed to the reduction of Fe^{3+} at exchanged sites to Fe^{2+}. The main peaks at 484 °C and the small shoulder at 435 °C should correspond to reduction of larger FeO_x particles [10,12–16]. Fe species located at the same sites should show similar H_2 reduction temperatures. Therefore, the first reduction peak for Fe-NaZ could be assigned to the reduction of Fe species located in ion exchange sites, similar to that seen for the dominating Fe species in Fe-HZ.

After hydrothermal deactivation, the H_2 consumption peaks of the aged samples were shifted to higher temperatures, implying a decease in the reducibility of active iron species in Fe-ZSM-5. Aged Fe-HZ showed a main peak at 405 °C while aged Fe-NaZ showed a main peak at 512 °C with a shoulder at 405 °C. According to Brandenberger *et al.* [10], the reduction peak of iron oxide clusters can shift to higher temperature with their size. The present H_2-TPR results indicate that the migration of Fe^{3+} from ion exchange sites and the formation of small FeO_x particles took place during the hydrothermal aging. Deconvolution of the H_2 consumption peaks (Fig. 1(b)) revealed that the percentage area of the first peak with respect to the total area of the H_2 consumption peaks was around 34% for both fresh and aged Fe-NaZ. This suggests that the degree of migration of Fe ions in Fe-ZSM-5 is mainly decided by their location in the zeolites.

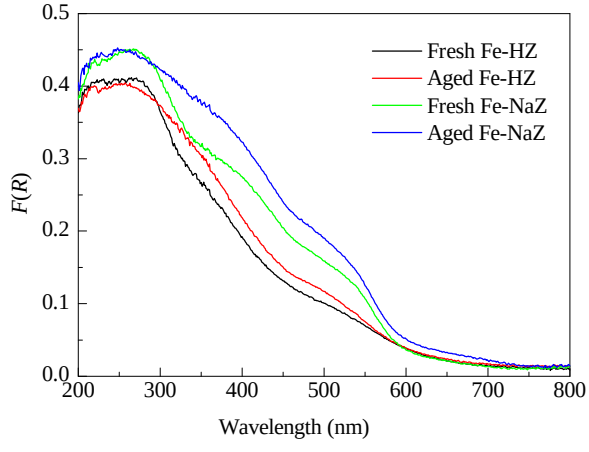

Fig. 2. UV-vis spectra of fresh and hydrothermally aged Fe-HZ and Fe-NaZ.

3.3. *UV-vis DRS results*

UV-vis DRS was used to study the distribution of Fe species in the Fe-ZSM-5 samples. The UV-Vis spectra of the fresh and aged Fe-ZSM-5 are compared in Fig. 2. Generally, the bands below 300 nm are assignable to isolated Fe^{3+} species located on ion exchange sites, while bands above 300 nm are assignable to oligomeric clusters (between 300–400 nm) and Fe_2O_3 particles (above 400 nm) [17,18]. As shown in Fig. 2, the spectra of Fe-NaZ exhibited a significant intensity of bands above 400 nm. In contrast, most of the peak bands of Fe-HZ were below 400 nm. To estimate the Fe species distribution in the catalyst, the UV-vis spectrum of each sample was deconvoluted with $r^2 > 0.999$, and the results are summarized in Table 1. From these data we obtained a rough estimation of the percentage of iso-

Table 1
Area percentages of sub-bands derived by deconvolution of the UV-vis DRS spectra.

Catalyst	I_1 (%)	I_2 (%)	I_3 (%)
Fresh Fe-HZ	50.2	31.7	18.1
Fresh Fe-NaZ	44.0	32.4	23.6
Aged Fe-HZ	46.9	33.7	19.4
Aged Fe-NaZ	40.6	34.1	25.3

I_1, I_2, and I_3 represent the percentage of isolated Fe^{3+} species (subbands at $\lambda \leq 300$ nm), oligmeric clusters (subbands at 300 nm $< \lambda <$ 400 nm), and Fe_2O_3 particles (subbands at $\lambda > 400$ nm), respectively.

lated Fe^{3+} species, oligomeric clusters, and Fe_2O_3 particles compared with the total Fe present in Fe-ZSM-5. The relative concentration of isolated Fe^{3+} species in Fe-HZ was found to be higher than that in Fe-NaZ, whereas Fe-NaZ contained more oligomeric Fe_xO_y clusters and Fe_2O_3 particles. After hydrothermal aging, the intensity of the bands above 300 nm increased, which indicates that hydrothermal aging caused the migration of isolated Fe^{3+} species from iron exchange sites and the formation of small clusters of iron oxides, which confirms the H_2-TPR results.

3.4. NH_3 adsorption

The in situ DRIFTS spectra of various samples measured after saturated NH_3 adsorption are shown in Fig. 3. The bands related to NH_3-adsorbed species appear at 3500–1400 cm^{-1} after NH_3 adsorption over Fe-ZSM-5. The bands related to NH_3 adsorbed species appearing at 3500–250 cm^{-1} can be assigned to the N–H stretching vibration of adsorbed NH_3 [14]. The band at 1480 cm^{-1} is assigned to the symmetric bending vibration of NH_4^+ chemisorbed onto Brønsted acid sites [14,17–20]. The negative band at 3610 cm^{-1} can be assigned to the OH stretch of Brønsted acid sites resulting from the interaction of surface hydroxyls with NH_3, which may reflect the relative concentration of Brønsted acid sites on the Fe-ZSM-5 [10,19–21]. The intensity of the band at 3610 cm^{-1} was higher for Fe-HZ than Fe-NaZ. A magnification of the 3610 cm^{-1} band is inset in Fig. 3. No IR bands corresponding to Brønsted acid sites were observed for Na-ZSM-5. Protonic sites can be introduced into Na-ZSM-5 by the ion exchange process [10,11]. The same bands were observed for fresh Fe-NaZ after NH_3 adsorption, but the intensity was lower compared with those observed for fresh Fe-HZ. After hydrothermal aging, the intensity of the negative band at 3610 cm^{-1} and the intensity of the bands of NH_3 adsorption species over Fe-HZ and Fe-NaZ were significantly decreased.

3.5. XRD and NMR results

Figure 4 shows the XRD patterns of the fresh and hydrothermally aged Fe-HZ and Fe-NaZ catalysts, and of a mechanical mixture of 5% α-Fe_2O_3 with H-ZSM-5 for comparison. The aged Fe-HZ and Fe-NaZ exhibited little change compared with those of the fresh samples. This indicates that the crystalline zeolite structure was retained after hydrothermal aging. The typical XRD peaks of α-Fe_2O_3 were observed at 33.1°, 35.6°, 40.9°, and 49.5° [14,22,23]. Low intensity peaks of α-Fe_2O_3 were detected in the XRD patterns of fresh and aged Fe-NaZ. This confirmed the presence of Fe_2O_3 particles in Fe-NaZ.

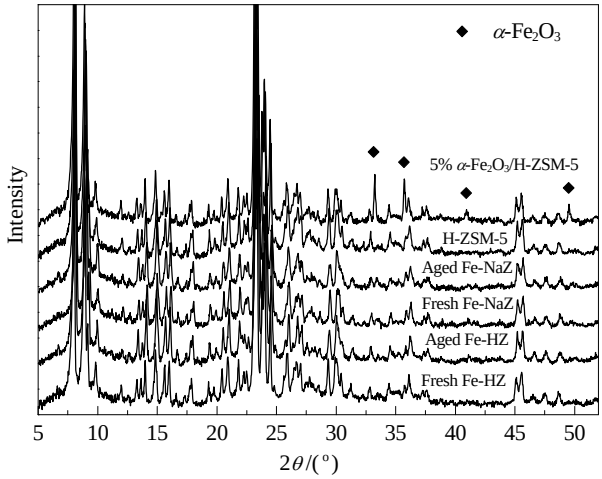

Fig. 4. XRD patterns of the different catalysts.

The ^{27}Al MAS NMR spectra of fresh and hydrothermally aged Fe-HZ and Fe-NaZ are shown in Fig. 5. The fresh Fe-ZSM-5 samples showed a strong signal at around 55 ppm, attributed to tetrahedrally coordinated aluminum, and a weak signal at around 0 ppm, assignable to octahedrally-coordinated aluminum (extra-framework) [10,24,25]. After hydrothermal aging, the intensity of the peak at 55 ppm was decreased owing to the removal of the aluminum from the tetrahedral zeolite framework. The intensity of the octahedral aluminum peak at 0 ppm was also decreased in the spectra of the aged samples. These results indicate that the aluminum removed from the tetrahedral zeolite framework was converted into distorted "NMR invisible" Al species [10,24]. The intensity of the tetrahedral

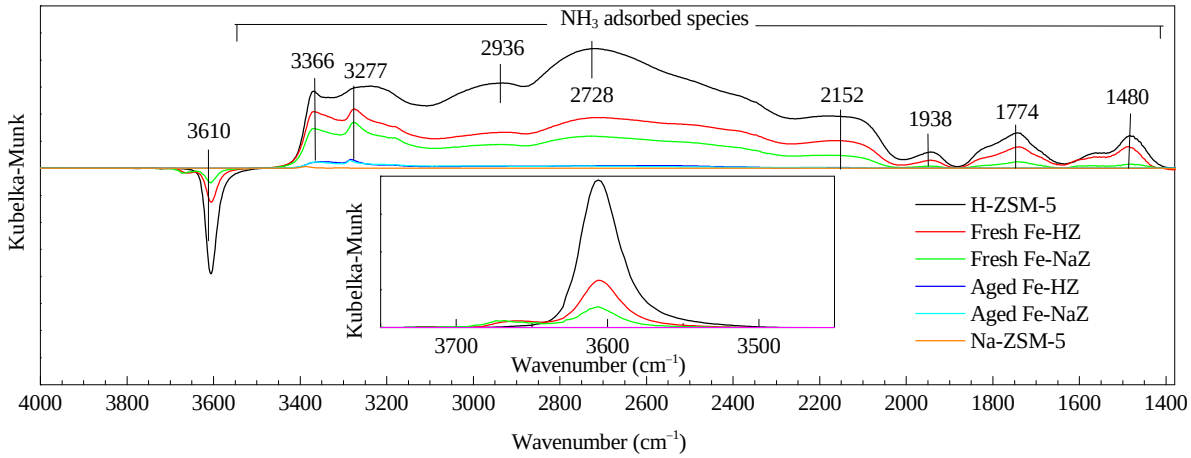

Fig. 3. DRIFTS spectra of NH_3 adsorbed over Fe-ZSM-5 catalysts (inset: magnification of the 3610 cm^{-1} band).

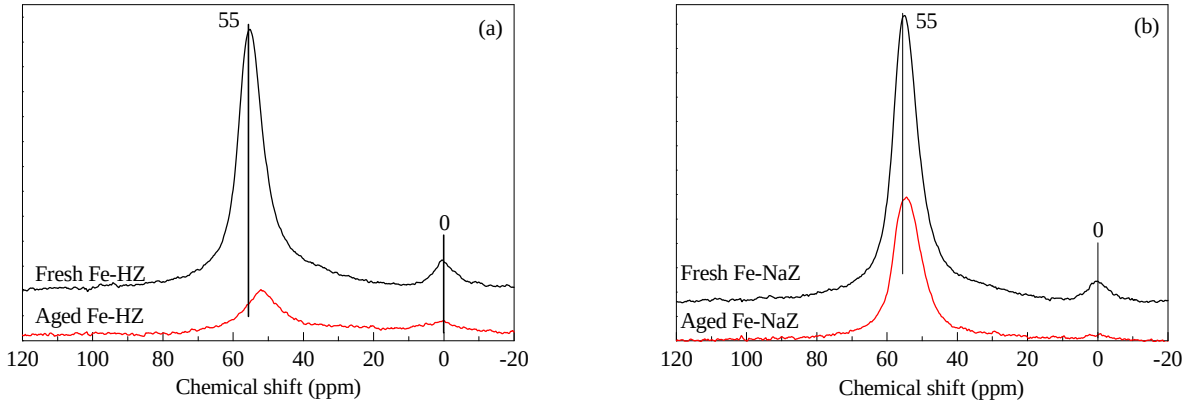

Fig. 5. Solid state ^{27}Al-NMR spectra of fresh and hydrothermally aged Fe-HZ (a) and Fe-NaZ (b).

aluminum peak in aged Fe-HZ more significantly was reduced than that of aged Fe-NaZ. The integrated peak area of the tetrahedral Al^{3+} ions in the aged samples was around 53% in Fe-NaZ and 26% in Fe-HZ. This indicates that the zeolite framework of Fe-NaZ was more stable during hydrothermal aging than that of Fe-HZ.

3.6. Catalytic activity

We conducted a comparative study of the effect of hydrothermal deactivation, and the presence of SO_2 and C_3H_6 on the SCR activity of the Fe-HZ and Fe-NaZ catalysts. Figure 6(a) shows NO_x conversion as a function of reaction temperature at 190–550 °C over fresh and hydrothermally aged Fe-HZ and Fe-NaZ catalysts. The fresh Fe-HZ showed higher SCR activity than the fresh Fe-NaZ within the whole reaction temperature range. Hydrothermal aging resulted in a significant decrease in NO_x conversion over the Fe-ZSM-5 catalysts, especially at low temperatures. The aged Fe-HZ also showed higher SCR activity than the aged Fe-NaZ.

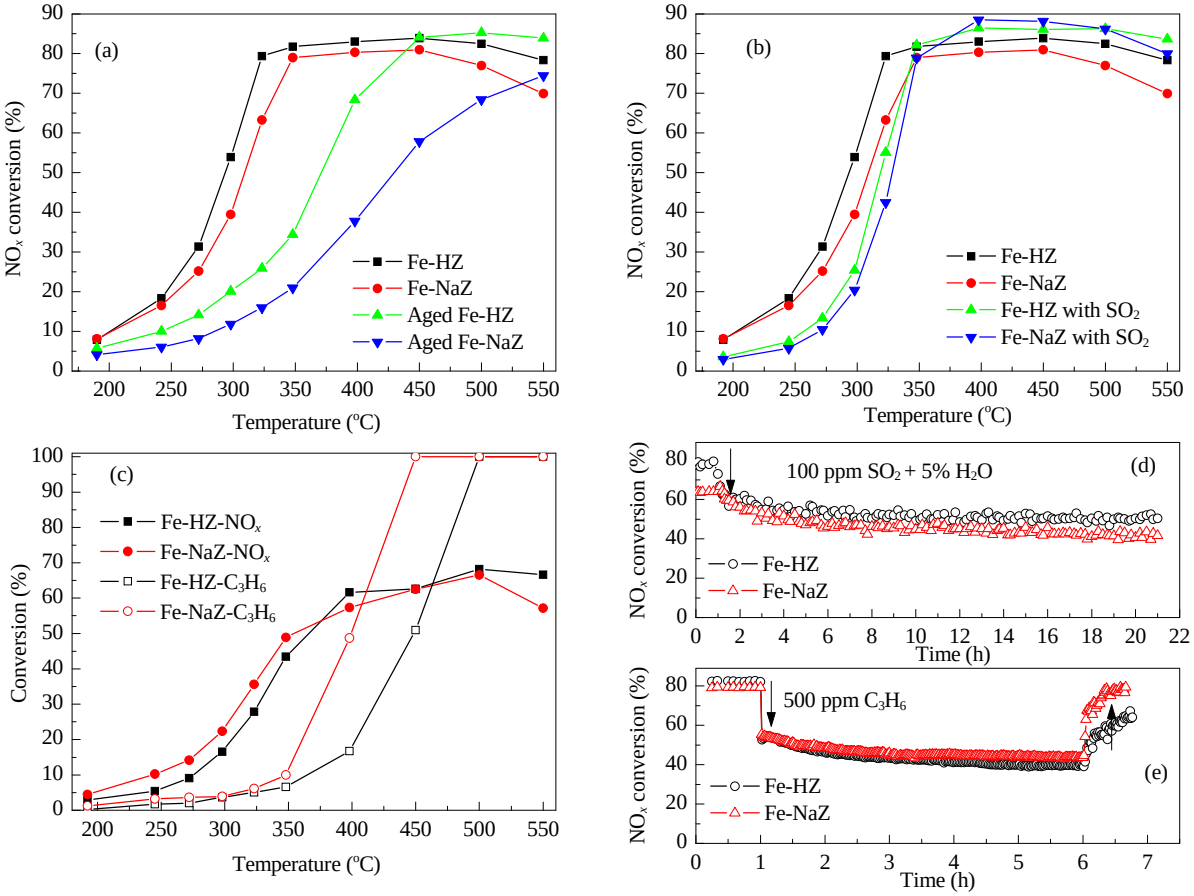

Fig. 6. SCR performance of Fe-ZSM-5 catalysts. (a) Hydrothermally deactivated; (b) Effect of SO_2; (c) Effect of C_3H_6; (d) SO_2 durability; (e) C_3H_6 durability.

The effect of SO_2 on the Fe-ZSM-5 catalysts is shown in Fig. 6(b). When 100 ppm SO_2 was added into the flue gas, a decline in NO_x conversion at low temperatures (below 350 °C) and a slight increase in NO_x conversion at high temperatures (>350 °C) were observed. The SO_2 durability (100 ppm) of Fe-HZ and Fe-NaZ was investigated at 325 °C with the copresence of 5% water (Fig. 6(d)). The SCR reaction was left to stabilize for 1 h before adding SO_2 and water. A sharp decline in the NO_x conversion of both the Fe-HZ and Fe-NaZ catalysts was observed upon addition of the SO_2 and water to the gas flow. The NO_x conversion of Fe-HZ was decreased from ca. 80% to ca. 55%, while that of Fe-NaZ was decreased from ca. 65% to ca. 45% after 20 h of reaction.

Figure 6(c) shows the NO_x and C_3H_6 conversions over Fe-HZ and Fe-NaZ in the presence of 500 ppm C_3H_6. The presence of C_3H_6 in the feed gas stream was found to resulted an apparent decrease in the NO_x conversion ability of both of the catalysts. Fe-NaZ exhibited higher NO_x conversion than Fe-HZ in the presence of C_3H_6. Fig. 6(e) shows the C_3H_6 durability of Fe-HZ and Fe-NaZ at 350 °C. After the SCR reaction had been stable for about 1 h, 500 ppm C_3H_6 was added to the reaction gas flow. The decrease in SCR activity caused by adding C_3H_6 was rapid in the first few minutes and then became slower in the time that followed. After 5 h reaction, the NO_x conversion of Fe-HZ decreased from 82% to 40% while that of Fe-NaZ decreased from 79% to 44%. It seems that the impact of C_3H_6 on the SCR activity was more significant for Fe-HZ than Fe-NaZ. When C_3H_6 was removed from the feed gas, the NO_x conversion of Fe-NaZ recovered within 20 min, while the NO_x conversion of Fe-HZ recovered slowly.

The SO_2-poisoned and C_3H_6-poisoned samples were regenerated after the durability tests by heating at 550 °C in air for 30 min. The regenerated catalysts were tested in the standard SCR reaction and the results were compared with those obtained for the fresh samples. As shown in Fig. 7, the NO_x conversions of the poisoned samples were partly recovered after the heat treatment. This indicates that the SO_2 and C_3H_6 poisoning of Fe-ZSM-5 was reversible. A better recovery of activity was observed for Fe-NaZ under the present regeneration conditions than Fe-HZ.

3.7. Discussion

The acidity and redox properties of Fe-ZSM-5 are two important parameters for the SCR reaction. The Brønsted acid sites of Fe-ZSM-5 are important for activating NH_3 species and are assumed to have a promoting effect for the SCR reaction at low temperatures [21,26]. Fe active sites are involved in the NO oxidation to NO_2, which is considered the slow step of the SCR reaction [22,27]. Among the various types of Fe species coexisting in the Fe-ZSM-5 catalysts, the isolated Fe^{3+} species are considered to contribute to the SCR reaction at low temperatures (< 300 °C) [23,28,29]. Therefore, the higher SCR activity of Fe-HZ might be mainly attributed to the higher amount of active Fe^{3+} ions and the greater number of Brønsted acid sites in this catalyst compared with those in Fe-NaZ.

The characterization results showed that hydrothermal aging of Fe-ZSM-5 catalysts led to the dealumination of the framework, the migration of Fe ions to form Fe_xO_y clusters, and a significant decrease in acidity, in accordance with previous reports [10,30]. Protons remaining on zeolites are well known to accelerate the process of steam-induced aluminum loss [10,11,15]. Fe-NaZ contained fewer protonic sites than Fe-HZ, so the dealumination of the zeolite framework by hydrothermal deactivation occurred to a much lesser extent for Fe-NaZ. The Brønsted acid sites of aged-Fe-HZ and aged-Fe-NaZ were significantly decreased to the point of almost completely disappearing. Therefore, the higher SCR activity of aged Fe-HZ should be attributed to the greater number of residual Fe^{3+} species located in the ion-exchanged sites of this catalyst. The loss of redox active Fe sites, rather than dealumination of zeolite framework, should be responsible for the decrease in SCR activity.

The impact of SO_2 on the SCR activity of Fe-ZSM-5 was different at low and high temperatures, in agreement with previous studies [31–33]. Long *et al.* [33] suggested that the formation of surface iron sulfate on Fe-ZSM-5 increased the surface acidity of the catalyst and resulted in enhancement of its high temperature activity. At low temperatures (< 325 °C), the formation of ammonium sulfite/sulfate might occur and cover some iron active sites, resulting in a decrease in SCR activity

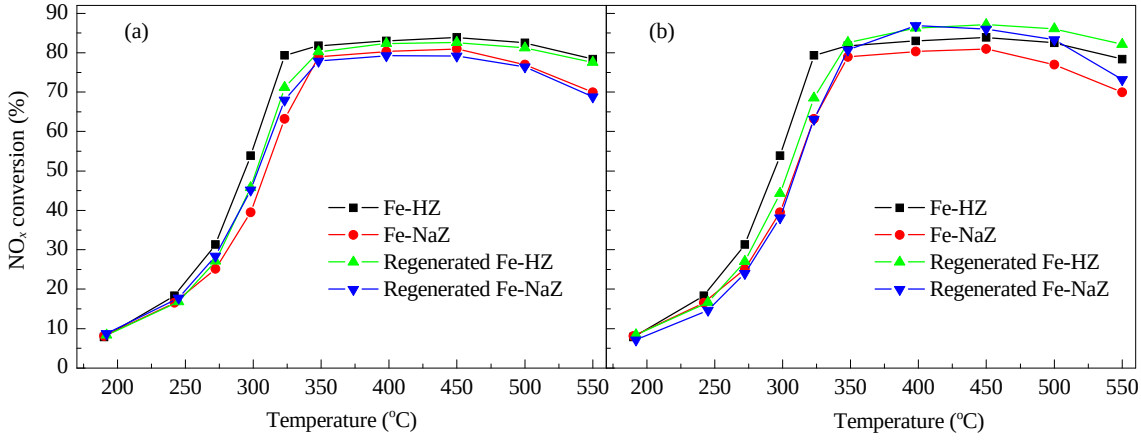

Fig. 7. SCR performance of fresh and regenerated Fe-ZSM-5. (a) After SO_2 durability test; (b) After C_3H_6 durability test.

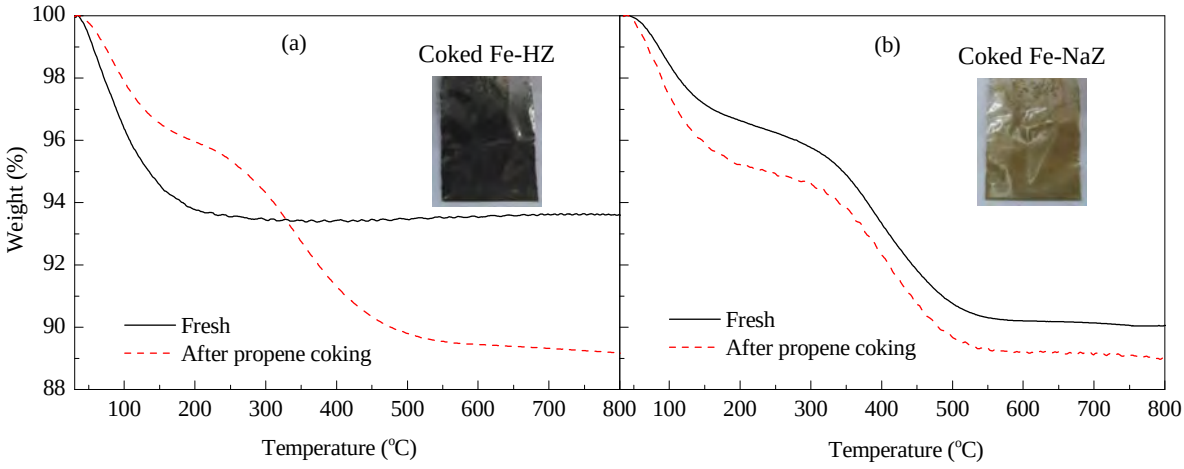

Fig. 8. Thermal analysis of Fe-HZ (a) and Fe-NaZ (b) as-prepared and after poisoning in 1000 ppm C_3H_6 at 200 °C.

[34]. The recovery of low temperature activity of Fe-ZSM-5 after regeneration can be explained as caused by the decomposition of these surface ammonium sulfite/sulfate species at high temperature.

Unburned hydrocarbons are always present in real exhaust gas. Zeolite SCR catalyst can be deactivated by hydrocarbons as a result of active site poisoning and pore blockage [35–39]. Pore blockage is known to mainly take place on acid sites [35–39]. The present Fe-HZ and Fe-NaZ catalysts were treated at 200 °C in 1000 ppm C_3H_6 in air for 4 h to obtain coked samples. The color of the coked Fe-HZ was dark brown, while that of the coked Fe-NaZ was a lighter brown (Fig. 8). Thermal analysis was carried out on the fresh and coked samples. When compared with those of the fresh catalysts, the mass loss of the HC-poisoned Fe-HZ was 4.7% higher, while that of the Fe-NaZ 1.2% was higher (Fig. 8). This indicates that more coke was formed on Fe-HZ compared with Fe-NaZ. Additionally, Fe-NaZ showed higher C_3H_6 conversion than Fe-HZ during SCR in the presence of C_3H_6 (Fig. 6(c)). Therefore, the better C_3H_6 poisoning resistance of Fe-NaZ should be attributed to less coking on the Fe-NaZ and the higher activity of C_3H_6 oxidation for this catalyst.

4. Conclusions

Fe-ZSM-5 catalysts prepared from H-ZSM-5 and Na-ZSM-5 showed differences in SCR activity, hydrothermal stability, and C_3H_6/SO_2 resistance owing to their different acidity and distributions of Fe species. The predominant Fe species in Fe-HZ was Fe^{3+} in ion exchanged sites, while Fe-NaZ contained a certain amount of Fe_2O_3 particles. The stability of these Fe^{3+} ions in Fe-ZSM-5 was mainly decided by their location. The zeolite structure of Fe-NaZ was more stable during hydrothermal aging than that of Fe-HZ. The presence of SO_2 and H_2O resulted in a decrease in the low temperature activity and an increase in the high temperature activity of both Fe-HZ and Fe-NaZ. Fe-NaZ showed better HC resistance than Fe-HZ, owing to less extensive hydrocarbon coking. Fe-HZ and Fe-NaZ deactivated by SO_2 or C_3H_6 was well regenerated by heating in air at 550 °C, although a better recovery of activity was observed for Fe-NaZ. According to the present results, to obtain better hydrothermal stability and hydrocarbon/SO_2 resistance, Fe-ZSM-5 catalysts should be prepared with greater quantities of Fe^{3+} species in ion exchanged sites and fewer residual protonic sites.

References

[1] Gabrielsson P L T. *Top Catal*, 2004, 28: 177
[2] Brandenberger S, Kröcher O, Tissler A, Althoff R. *Catal Rev*, 2008, 50: 492
[3] Park J H, Park H J, Baik J H, Nam I S, Shin C H, Lee J H, Cho B K, Oh S H. *J Catal*, 2006, 240: 47
[4] Long R Q, Yang R T. *J Am Chem Soc*, 1999, 121: 5595
[5] Torre-Abreu C, Ribeiro M F, Henriques C, Delahay G. *Appl Catal B*, 1997, 14: 261
[6] Coq B, Delahay G, Durand R, Berthomieu D, Ayala-Villagomez E. *J Phys Chem B*, 2004, 108: 11062
[7] Sultana A, Nanba T, Haneda M, Hamada H. *Catal Commun*, 2009, 10: 1859
[8] Sultana A, Nanba T, Haneda M, Sasaki M, Hamada H. *Appl Catal B*, 2010, 101: 61
[9] Sullivan J A, Keane O. *Appl Catal B*, 2005, 61: 244
[10] Brandenberger S, Kröcher O, Casapu M, Tissler A, Althoff R. *Appl Catal B*, 2010, 101: 649
[11] Pieterse J A A, Pirngruber G D, van Bokhoven J A, Booneveld S. *Appl Catal B*, 2007, 71: 16
[12] Krishna K, Seijger G B F, van den Bleek C M, Makkee M, Mul G, Calis H P A. *Catal Lett*, 2003, 86: 121
[13] Chen H, Sachtler W M H. *Catal Today*, 1998, 42: 73
[14] Qi G, Yang R T. *Appl Catal B*, 2005, 60: 13
[15] Lee H T, Rhee H K. *Catal Lett*, 1999, 61: 71
[16] Lobree L J, Hwang I, Reimer J A, Bell A T. *J Catal*, 1999, 186: 242
[17] Brandenberger S, Kröcher O, Tissler A, Althoff R. *Appl Catal A*, 2010, 373: 168
[18] Kumar M S, Schwidder M, Grünert W, Brückner A. *J Catal*, 2004, 227: 384
[19] Castoldi L, Bonzi R, Liett L, Forzatti P, Morandi S, Ghiotti G, Dzwigaj S. *J Catal*, 2011, 282: 128
[20] Eng J, Bartholomew C H. *J Catal*, 1997, 171: 27
[21] Brandenberger S, Kröcher O, Wokaun A, Tissler A, Althoff R. *J Catal*, 2009, 268: 297

Graphical Abstract

Chin. J. Catal., 2015, 36: 649–656 doi: 10.1016/S1872-2067(14)60268-0

The effect of Fe species distribution and acidity of Fe-ZSM-5 on the hydrothermal stability and SO_2 and hydrocarbons durability in NH_3-SCR reaction

Xiaoyan Shi*, Hong He, Lijuan Xie
Research Center for Eco-Environmental Sciences, Chinese Academy of Sciences

Fe-ZSM-5 prepared from Na-ZSM-5 is more stable against hydrothermal deactivation and shows better SO_2 and C_3H_6 poisoning resistance than Fe-ZSM-5 prepared from H-ZSM-5.

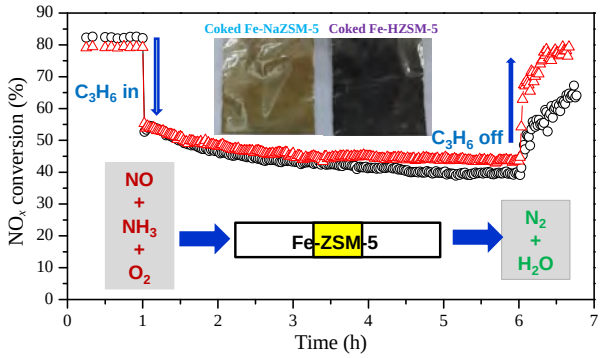

[22] Delahay G, Valade D, Guzmán-Vargas A, Coq B. *Appl Catal B*, 2005, 55: 149
[23] Iwasaki M, Yamazaki K, Banbo K, Shinjoh H. *J Catal*, 2008, 260: 205
[24] Iwasaki M, Shinjoh H. *Phys Chem Chem Phys*, 2010, 12: 2365
[25] Cheng Y, Hoard J, Lambert C, Kwak J H, Peden C F F. *Catal Today*, 2008, 136: 34
[26] Schwidder M, Kumar M S, Bentrup U, Pérez-Ramírez J, Brückner A, Grünert W. *Microporous Mesoporous Mater*, 2008, 111: 124
[27] Long R Q, Yang R T. *J Catal*, 2002, 207: 224
[28] Brandenberger S, Kröcher O, Tissler A, Althoff R. *Appl Catal B*, 2010, 95: 348
[29] Høj M, Beier M J, Grunwaldt J D, Dahl S. *Appl Catal B*, 2009, 93: 166
[30] Shi X Y, Liu F D, Shan W P, He H. *Chin J Catal*, 2012, 33: 454
[31] Ma A Z, Grünert W. *Chem Commun*, 1999: 71
[32] Long R Q, Yang R T. *J Catal*, 1999, 188: 332
[33] Long R Q, Yang R T. *J Catal*, 2000, 194: 80
[34] Kim Y J, Kwon H J, Heo I, Nam I S, Cho B K, Choung J W, Cha M S, Yeo G K. *Appl Catal B*, 2012, 126: 9
[35] Heo I, Lee Y, Nam I S, Choung J W, Lee J H, Kim H. *Microporous Mesoporous Mater*, 2011, 141: 8
[36] He C H, Wang Y H, Cheng Y S, Lambert C K, Yang R T. *Appl Catal A*, 2009, 368: 121
[37] Li J H, Zhu R H, Chen Y S, Lambert C K, Yang R T. *Environ Sci Technol*, 2010, 44: 1799
[38] Ma L, Li J H, Cheng Y S, Lambert C K, Fu L X. *Environ Sci Technol*, 2012, 46: 1747
[39] Malpartida I, Marie O, Bazina P, Daturia M, Jeandel X. *Appl Catal A*, 2011, 102: 190